Research Annals of Industrial and Systems Engineering

www.raise.reapress.com

Res. Ann. Ind. Syst. Eng.Vol. 2, No. 1 (2025) 48–71.

Paper Type: Original Article

Estimation of Route Reliability in Multimodal Hierarchical Hub Location Problem Using Lagrangian Relaxation and Artificial Neural Networks (ANN)

Ehsan Korani*

Department of Industrial Engineering, Kermanshah Branch, Islamic Azad University, Kermanshah, Iran; Ehsan.Korani@iau.ac.ir.

Citation:

Received: 01 August 2024 *Revised: 12 October 2024* *Accepted: 11 December 2024*	Korani, E. (2025). Estimation of route reliability in multimodal hierarchical hub location problem using lagrangian relaxation and artificial neural networks (ANN). *Research annals of industrial and systems engineering, 2*(1), 48-71.

Abstract

The present study has developed an Artificial Neural Networks (ANN) model to predict the route reliability in various structures of the Multimodal Hierarchical Hub Location Problem (MHHLP) utilizing Lagrangian relaxation; so that, initially, a mixed integer programming model was proposed for MHHLP and the, an efficient Lagrangian relaxation method was developed to solve the problem in different structures. The results obtained from problem solving were used as input and output data to create an ANN model using Multilayer Perceptron (MLP) neural network. As a result, an ANN model was designed by which, the reliability of the MHHLP route was predicted in large dimensions at different values of the parameters. Computational analysis, ANN model validation and prediction process were conducted using CAB and IAD data.

Keywords: Hub location problem, Lagrangian relaxation, Artificial neural networks, Reliability, Hierarchical.

1 | Introduction

Hub Location Problems (HLPs) which are known as "network optimization problems", identify hubs as collection and distribution centers [1]. In these problems, less and more direct connections are used to achieve the economic interests rather direct relationship between the two points and accordingly, demands with the same destination are aggregated and then distributed.

There are various other applications in the HLPs in addition to telecommunication and transportation systems, including production planning, retail management, wholesale management, and healthcare.

Teo and Shu [2-15] and many other works have been conducted in this field. However, along with the issues raised in all of these problems with a wide variety of applications, it should be noted that the disruption and revocation of a service flow will impose additional costs in addition to unfulfilled economic goal. The costs

Corresponding Author: Ehsan.Korani@iau.ac.ir
https://doi.org/10.22105/raise.v2i1.37

include increased direct and indirect costs, intensified dissatisfaction, and undermined system legitimacy [4]. Therefore, the reliability of the network communication routes and how to establish hub facilities based on reliability is important. However, Snyder et al. [16] have considered the effects of natural disasters, labor strikes, or terrorist threats among the factors affecting the reliability. The importance of this issue is increasing day by day by growing the industrial society and the increased volume of communications, and the growth of scientific research is possible in the field of reliable hub location. Kim and O'kelly [17] were the first ones who focused on promoting the reliability of communication routes in the hub location problem and An et al. [4] improved the hub facility reliability factor by defining the backup facilities. According to them, given the strategic level of HLPs, the solving method is of great importance. Therefore, they proposed two approaches of branch and bound and Lagrangian for their model.

One of these characteristics of the HLPs is the hierarchical structure proposed by Yaman [18], Alumur et al. [10] and Korani and Sahraeian [13]. However, multimodal transportation is another important characteristic that has been taken today beyond hub problems in the field of macro transportation. Competition in the field of accelerated services is one of the key indicators of global trade, led to inefficiencies in specialized and individual transportation [19]. Therefore, emphasis on multimodal transportation in hub has also been important as can be observed in recent research including Chen et al. [20], Alumur et al. [14], Onyemechi [21], SteadieSeifi et al. [22], Hanasusanto et al. [23], Ambrosino and Sciomachen [24], Fazayeli et al. [25] and Huang et al. [26]. However, simultaneous emphasis to these three characteristics causes new contingencies that should be considered in designing the model.

Given the complexity and time-consuming nature of the solving process of various problems in the real world, researchers have tried to overcome these complexities by creating new methods. One of these methods is the Artificial Neural Network (ANN), which is more useful than many models, and this is because of their higher level of speed and accuracy [27–29]. By the motivation of developing an alternative model that allows for a quick and reliable estimation of site overhead costs, Leśniak and Juszczyk [29] suggested an ANN-based regression model which was able to predict the site overhead cost index.

A new method for quick and accurate estimation and forecasting iron oxide (FeO) concentration in steel slag during discharge process in steelworks was also proposed utilizing two key tools of the ANN and infrared imaging [30]. This method has attempted to estimate and predict the value of material physical parameters based on the changes in the radiative parameters, which is most relevant to the amount of FeO in steel production.

An ANN model based on the input parameters of random data and strain values obtained from the static test was proposed to predict the static load applied on the wing rib [31]. The performance of their proposed ANN model has been also evaluated in predicting static load to a degree of accuracy.

Continuous and permanent monitoring of Particulate Matter (PM) at subway station is of particular importance for assessing the exposure level of PM to passengers. In this way, PM variations were predicted using ANN for 6 subway stations in Seoul. This ANN model has three inputs of outdoor PM10 concentrations, ventilation rates, and subway frequencies in the input layer, a hidden layer and an output layer [32].

Optimizing the design process of asphalt mix in the road construction industry is one of the interesting uses of ANN which used by Sebaaly et al. [33] to optimize the asphalt mix design process using past process database suggesting a mixed method of ANN and Genetic Algorithm, so that their results were consistent with the applicable specification requirements.

ANN was also used in a heuristic effort to estimate the operatinal parameters of the counter-rotating wind turbine in which, neural networks played an important role in enabling the optimization of the dual-rotor turbine parameters [34].

An ANN model was used to model air void content in an aggregate mixture, which was designed for feed-forward type using the error Back-Propagation Algorithm (BPA) [35].

ANN has also been used to predict gold price fluctuations, so that Kristjanpoller and Minutolo [36] presented a hybrid model of ANN and the generalized autoregressive conditional hetero-skedasticity (GARCH), which also analyzed the price fluctuations of the gold spot price and future price. This mixed model dramatically contributed to predict the process in order to determine the impact of financial variables on gold prices.

ANN has also been considered in the field of agricultural industry, so that it has been used to predict the amount of sesame seed production. The prediction in this process was utilized two models of ANN and Multiple Regression Models (MLRs) that eventually, ANN prediction outcomes were far better than the MLR results based on the comparison results [37].

There are many instances of ANN application in literature; however the lack of the Location-Allocation Problems (LAPs) is so clear in literature. Hence, it is attempted in this paper, to implement ANN in the HLPs (as one of the LAPs subsets).

HLPs fall into the NP-Hard problems group [38], and increased reliability aspects of these problems causes doubling their complexity, and reliable HLPs can be surely placed in this group. So, the Lagrangian relaxation solution is used in the problem solving process. Accordingly, different algorithms and methods for these problems spend considerable time to solution to provide final result and problem solution. For instance, sometimes it is needed to compare the solution and select it from a set of solutions of the problem to select the final solution so that each solution is obtained by changing the problem parameters and re-executing the solving method, which requires considerable time. In this paper, we attempted to provide a linear modeling of Multimodal Hierarchical Hub Location Problem (MHHLP), utilizing ANN that provides a set of the problem different solutions for different values of parameters with a minimum error rate and in the least possible time.

Therefore, the most important contribution of this paper is designing and developing an ANN linear model to predict the objective function of problem, in addition to provide a multimodal hierarchical hub location model and developing the lagrangian relaxation algorithm for its solution process.

The reminder of the paper is structured as follows according to the well-known patterns in the literature: the problem statement and the mathematical model are presented in Section 2. The steps of solving the lagrangian relaxation are presented in Section 3. Section 4 describes the design stages of the ANN model. Section 5 describes the computational results and MHHLP route reliability prediction stages. Finally, conclusion and research suggestions are provided in Section 6.

2|MHHLP Formula

As mentioned earlier, the MHHLP research problem is one of the specific problems and subsets of LAPs. Therefore, before designing the mathematical model of the problem, first, its assumptions will be described to determine how the model will be formed. Then various indices and sets are introduced, after which the parameters and variables of the problem are presented. Finally, the integer programming model is proposed.

2.1|MHHLP Assumptions

In this model, the costs of the investment are somehow minimized in terms of affecting the flow rate of each route in the objective function and the make dependencies between the routes reliability on the traveled distance. This is because of the logic that the shorter route has a less probability of disruption, and the possibility of disconnecting is far less than the longer route.

The MHHLP problem to solve the reliability is related to the volume of traffic and the distance traveled to calculate reliability, so it has specific computational properties.

The following assumptions are proposed for the mathematical model:

I. The hubbing effect is considered as constant values, between 0 and 1, as the discount factor at different levels of the hub network.

II. The problem has three-level. The first level is related to the non-hub nodes, the second level is related to facilities hub, and the third level is related to facilitating the central hub (see also Yaman [18], Korani and sahraeian [9]).

III. The hierarchical structure of the output network is in nested and non-coherent form.

IV. The transportation mode is ground between the hub and non-hub and air between the air hub and the central hub.

V. The number of hub facilities is constant in each level and the problem approach is p-hub.

VI. The facilities location-allocation optimization problem approach is implemented.

VII. Facilities capacity and transmission routes are unconstrained.

VIII. The time to travel between the nodes and the demand values is constant.

IX. The first level has a central hub facility.

X. The location of the demand nodes is predetermined.

XI. The hub facilities potential locations are known.

XII. The solution space is discrete.

2.2 | Indices and Symbols Of MHHLP

In this section, the three components of the model, namely sets, parameters, and variables of the problem have been introduced. The indices used in the proposed model include:

I: the set of all studied nodes.

H: the set of the potential nodes of the hub ($H \subseteq I$).

C: the set of the potential nodes of the central hub ($C \subseteq H$).

Parameters:

P_H : the number of hub facilities in the second level.

f_{ij} : the demand flow rate between the source $i \in I$ and the destination $j \in I$.

α: discount factor of hubbing effect on transportation time ($0 \leq \alpha < 1$).

γ : the impact factor of hubbing effect on the reliability ($0 \leq \gamma < 1$).

β: maximum time to service between each pair of source and destination nodes.

t_{ij} : travel time in the communication route between $i \in I$ and $j \in I$ nodes in ground transportation mode.

$\bar{t}_{ij}$: travel time in the communication route between the $i \in I$ and $j \in I$ nodes in the air transportation mode.

r_{ij} : the reliability of the communication route between $i \in I$ and $j \in I$ nodes in the ground transportation mode.

$\bar{r}_{ij}$: the reliability of the communication route between $i \in I$ and $j \in I$ nodes in the air transportation mode.

Variables:

x_{ikl} : 1 If the node is assigned to the hub $k \in H$ and is assigned to the central hub $l \in C$ through this hub, 0, otherwise, the node $k \in H$ is a hub in the second level if $x_{kkl} = 1$. Also, the central hub is established in the node $l \in C$ if $x_{lll} = 1$.

z_{kl}^{i} : the flow rate derived from the source node $i \in I$ passing through the communication route between the hub node $k \in H$ and the central hub $l \in C$ node.

y_{ij}^{m} : the flow rate derived from the source node $i \in I$ that reaches the destination node j ∈ I through the hub $m \in H$.

T_l : maximum time needed by each demand flow to reach the central hub $l \in C$ node.

w_{ij}^{km} : the flow rate derived from the source node $i \in I$, which arrives at the destination node $j \in I$ through the route where two distinct hubs of k and m are located, so w_{ij}^{km} is quantifiable when $x_{ikl} = 1$.

2.3 | Mathematical Formulation of MHHLP

An example is presented in *Fig. 1* to describe the problem, in which there are 8 demand nodes. The nodes k, l, and m are the second level hub and the central hub l node (given the nested feature of the node l is both a hub and a central hub, see also; Yaman [18]; Koran and Sahraeian [13], so, there are four general routes. The route of type 1 occurs when there is only one hub in the route, and moving from the non-hub node to the hub or central hub node, the routes i→k, e→l, j→m, and q→m are the route of type 1. The route of type 2 occurs when a hub is in the route, but the flow starts from the hub to the non-hub node, the inversed flow of the four paths of type 1, e→l→u, q→m→j and the inverse of these two routes is of Type 2. Route 3 is a path with a hub and a central hub, with the direction of the hub to the central hub, the routes m→l and i→k→l are of this type. The route 4 occurs when there is more than one hub in the route and the flow passes through the central hub, so multiple scenarios are created. The routes i→k→l→e, k→l→e , e→l→m→j , e→l→m , l→m , l→m→j , k→l→m , k→l→m→j , i→k→l→m and i→k→l→m→j are of this kind. It should be noted that in these routes, the initial node transfers its demand (ie. fij) to the final node through the intermediate nodes and the demand flow of the other nodes are not involved in these routes.

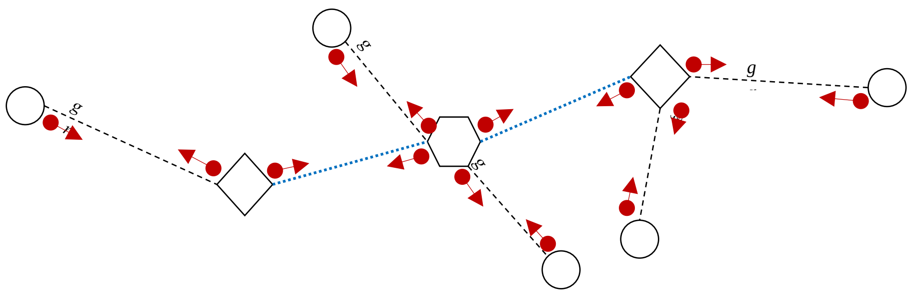

Fig. 1. Hierarchical hub network with 8 demand nodes, 3 hubs and a central hub.

We considered the communication mode between the hub and non-hub nodes as ground and the between hub and central hub nodes as air on this multimodal route, followed by Alumur et al. [10]. Thus, according to what mentioned above, how to calculate the reliability of the routes in figure 1 is calculated in *Table 1*, which is applied to air routes with an impact factor on reliability (γ). It should be noted that for each $i \in I$, $r_{ii} = 1$ since the chance of reaching a node to itself is deterministic.

Table 1. The reliability of the flow passing through each of the four paths.

Route	Flow Reliability	No.	Route	Flow Reliability	No.
i→k	$r_{ik} x_{ikl} \sum_{j\in H} f_{ij}$	1	i→k→l→m→j, $k \neq m$	$r_{ik} \overline{r}_{kl}^{\gamma} \overline{r}_{lm}^{\gamma} r_{mj} w_{ij}^{km}$	4
e→l	$r_{el} x_{ill} \sum_{j\in I} f_{ej}$	1	i→k→l→e, $k \neq l$	$r_{ik} \overline{r}_{kl}^{\gamma} \overline{r}_{ll}^{\gamma} r_{le} w_{ie}^{kl}$	4
i→k→l	$r_{ik} \overline{r}_{kl}^{\gamma} z_{kl}^{i}$	3	u→l→m→j, $l \neq m$	$r_{ul} \overline{r}_{ll}^{\gamma} \overline{r}_{lm}^{\gamma} r_{mj} w_{uj}^{lm}$	4
q→m→j, $m \neq j$	$r_{qm} r_{mj} w_{qj}^{mm}$	2	e→l→u, $l \neq u$	$r_{el} r_{lu} x_{ell} y_{eu}^{l}$	2

Now, the objective function of the problem with the goal of maximizing the reliability of the flow of the network paths, is proposed as *Eq. (1)* according to *Table 1*.

$$\mathrm{Max} \sum_{i\in I}\sum_{k\in H}\sum_{l\in C} r_{ik} x_{ikl} \sum_{j\in I} f_{ij} + \sum_{i\in I}\sum_{k\in H}\sum_{l\in C} r_{ik} \overline{r}_{kl}^{\gamma} z_{kl}^{i} + \sum_{i\in I}\sum_{k\in H\setminus\{j\}}\sum_{j\in I} r_{ik} r_{kj} w_{ij}^{kk} + \sum_{i\in I}\sum_{k\in H}\sum_{m\in H\setminus\{k\}}\sum_{l\in C} r_{ik} \overline{r}_{kl}^{\gamma} \overline{r}_{lm}^{\gamma} r_{mj} w_{ij}^{km}. \tag{1}$$

The objective function formulate in four parts of *Models (1-1), (1-2), (1-3)* and *(1-4)*, so, we breakdown to explain one by one as follow:

$$\sum_{i\in I}\sum_{k\in H}\sum_{l\in C} r_{ik} x_{ikl} \sum_{j\in I} f_{ij}. \tag{1-1}$$

$$\sum_{i\in I}\sum_{k\in H}\sum_{l\in C} r_{ik} \overline{r}_{kl}^{\gamma} z_{kl}^{i}. \tag{1-3}$$

$$\sum_{i\in I}\sum_{k\in H\setminus\{j\}}\sum_{j\in I} r_{ik} r_{kj} w_{ij}^{kk}. \tag{1-2}$$

$$\sum_{i\in I}\sum_{k\in H}\sum_{m\in H\setminus\{k\}}\sum_{l\in C} r_{ik} \overline{r}_{kl}^{\gamma} \overline{r}_{lm}^{\gamma} r_{mj} w_{ij}^{km}. \tag{1-4}$$

According to *Table 1*, we encounter four types of routes 1-4, so the objective function in the form of four sections *Models* (*1-1), (1-2), (1-3)*, and *(1-4)* is described for the route types 1 to 4, respectively. Problem constraints are grouped based on the structure created in the problem, as follows:

Single assignment hub location-allocation

The constraints of the hub network structure are designed as single assignment in this section. *Constraint (2)* ensures that each demand node has only one route to the central hub. *Constraint (3)*, *Constraint (4)*, and *Constraint (6)* are only allowed to establish the route when the middle node being a hub or central hub. *Constraint (5)* and *Constraint (6)* reinforce the single assignment structure.

$$\sum_{k\in H}\sum_{l\in C} x_{ikl} = 1, \quad \text{for all } i \in I. \tag{2}$$

$$x_{ikl} \leq x_{kkl}, \qquad \text{for all } i \in I, k \in H, l \in C, k \neq i. \tag{3}$$

$$\sum_{m\in H} x_{kml} \leq x_{lll}, \qquad \text{for all } k \in H, l \in C, l \neq k. \tag{4}$$

$$x_{lkl} = 0, \quad \text{for all } k \in H, l \in C, l \neq k. \tag{5}$$

$$x_{ikl} \in \{0,1\}, \quad \text{for all } i \in I, k \in H, l \in C. \tag{6}$$

Opening P-hub facilities:

Considering that the design basis for the P-hub median problem and the number of facilities to be established are given at each level, *Constraint (7)* and *Constraint (8)* determine the number of hub facility in the second level and the number of central hub to be established at first level.

$$\sum_{j\in H}\sum_{l\in C} x_{jjl} = p_H. \tag{7}$$

$$\sum_{l\in C} x_{lll} = 1. \tag{8}$$

Flow balance constraints:

$$z_{kl}^i \geq \sum_{j\in I: j\neq k} (f_{ij}+f_{ji})(x_{ikl}-x_{jkl}), \quad \text{for all } i\in I, k\in H, l\in C, l\neq k. \tag{9}$$

$$\sum_{k\in H}\sum_{l\in C} z_{kl}^i \leq \sum_{j\in I}(f_{ij}+f_{ji}), \quad \text{for all } i\in I. \tag{10}$$

$$\sum_{i\in I} y_{ij}^k \leq x_{jkl}\sum_{i\in I} f_{ij}, \quad \text{for all } j\in I, k\in H, l\in C. \tag{11}$$

$$\sum_{k\in H} y_{ij}^k = f_{ij}, \quad \text{for all } i\in I, j\in I. \tag{12}$$

$$w_{ij}^{km} \leq x_{ikl}\sum_{a\in I} f_{ia}, \quad \text{for all } i\in I, k\in H, l\in C, m\in H, j\in I. \tag{13}$$

$$w_{ij}^{km} \leq y_{ij}^m, \quad \text{for all } i\in I, k\in H, m\in H, j\in I. \tag{14}$$

$$w_{ij}^{km} \geq y_{ij}^m - (1-x_{ikl})\sum_{a\in I} f_{ia}, \quad \text{for all } i\in I, k\in H, l\in C, m\in H, j\in I. \tag{15}$$

$$w_{ij}^{km} \geq 0, \quad \text{for all } i\in I, k\in H, l\in C, m\in H, j\in I. \tag{16}$$

$$z_{kl}^i \geq 0, \quad \text{for all } i\in I, k\in H, l\in C. \tag{17}$$

$$y_{ij}^k \geq 0, \quad \text{for all } i\in I, j\in I, k\in H. \tag{18}$$

Constraint (9) calculates the amount of output flow from the source node i, passing the hublink between the hub k and the central hub l. This constraint is used as balancing constraint in Yaman [18] and Korani and Sahraeian [9] Used.

Hence for every link from a hub to its central hub, the amount of traffic demand will be computed by *Constraint (9)* and *Constraint (10)*.

Constraint (10) ensures that the variable flow rate originating from source i, passing through the connecting route of the nodes of the hub k and the central hub l, is not greater than the total flow derived from the source node i. This constraint is introduced in Correia et al. [39] according to its application. The *Constraint (11)* and *Constraint (12)* are designed inspired by Ernst & kirshnamoorthy [40] and Karimi and setak [11], that guarantee that the target node j receives a flow originating from the source node i. The *Constraint (13)* and *Constraint (14)* guarantee that when the demand flow is transferred from the source node i to the destination node j through two hubs k and m, respectively, the nodes i are assigned to the hub k and node j to the m hub. The *Constraints (15)* are also applied to ensure the accuracy level of flow rate. The *Constraints (16)-(18)* amplify the LP model.

$$\sum_{k\in H}(t_{ik}+\alpha\ \bar{t}_{kl})x_{ikl} \leq T_l, \quad \text{for all } i\in I, l\in C. \tag{19}$$

$$T_l + \sum_{r\in H}(\alpha\ \bar{t}_{lr}+t_{rj})x_{jrl} \leq \beta, \quad \text{for all } j\in I, l\in C. \tag{20}$$

$$T_l \geq 0, \quad \text{for all } l\in C. \tag{21}$$

Constraints (19)-(21) indicate the time bound constraints. These constraints guarantee that the travel time between each pair of source and destination nodes is no greater than the predetermined value of β. *Constraint (19)* serves travel time from each source to the central hub of that node in the variable, and the *Constraint (20)* places the total travel time from the source node to the destination node under the radius of the upper bound of β. The idea of this set of constraints in derived from research such as Ebery [41], Ernst et al. [42], Yaman [18] and Korani and Sahraeian[9].

3 | Lagrangian Relaxation Method

There are various approaches based on mathematics to simplify the model and relax it from the variables and constraints that make the problem difficult to solve, including the Lagrangian relaxation method which is developed for the MHHLP model in the present paper. This methodology has been developed for several models in the HLPs literature including Aykin [43], Lee et al. [44], Marín [45], Contreras et al. [46], Ishfaq and Sox [47], Mohammadi et al. [48], Karimi and Setak [11], He et al. [49] and Neamatian Monemi et al. [5].

According to the literature, the problem constraints was identified, and it was observed that the relationship between the two decision variables x_{ikl} and w_{ij}^{km} dramatically affect the time to solution which was observed in *Constraint (13)* and *Constraint (15)*. Hence, two sets of Lagrange multipliers λ_{ij}^{km} and μ_{ij}^{km} were defined for the *Constraint (13)* and *Constraint (15)*, respectively ($\lambda_{ij}^{km} \geq 0$ and $\mu_{ij}^{km} \geq 0$). With the help of Lagrange multipliers, the relaxed problem as LR was defined as *Eq. (22)*.

$$
\begin{aligned}
LR(\bar{\lambda},\bar{\mu}):\text{Max} & \sum_{i\in I}\sum_{k\in H}\sum_{j\in I\backslash\{k\}} r_{ik}r_{kj}w_{ij}^{kk} + \sum_{i\in I}\sum_{k\in H}\sum_{m\in H\backslash\{k\}}\sum_{j\in I}\sum_{l\in C} r_{ik}\bar{r}_{kl}^{\gamma}\bar{r}_{lm}^{\gamma}r_{mj}w_{ij}^{km} + \sum_{i\in I}\sum_{k\in H}\sum_{l\in C}(r_{ik}x_{ikl}\sum_{j\in I}f_{ij} + r_{ik}\bar{r}_{kl}^{\gamma}z_{kl}^{i}) \\
& -\sum_{i\in I}\sum_{k\in H}\sum_{m\in H}\sum_{j\in I}\mu_{ij}^{km}y_{ij}^{m} + \sum_{i\in I}\sum_{k\in H}\sum_{m\in H}\sum_{j\in I}\mu_{ij}^{km}w_{ij}^{km} + \sum_{i\in I}\sum_{k\in H}\sum_{m\in H}\sum_{j\in I}\sum_{l\in C}\mu_{ij}^{km}(1-x_{ikl})\sum_{a\in I}f_{ia} \\
& -\sum_{i\in I}\sum_{k\in H}\sum_{m\in H}\sum_{j\in I}\lambda_{ij}^{km}w_{ij}^{km} + \sum_{i\in I}\sum_{k\in H}\sum_{m\in H}\sum_{j\in I}\sum_{l\in C}\lambda_{ij}^{km}x_{ikl}\sum_{a\in I}f_{ia}.
\end{aligned} \tag{22}
$$

Such that. (2)-(12),(14),(16) and (21)

The problem $LR(\bar{\lambda},\bar{\mu})$ is a formulation based on the Lagrangian relaxation approach, resulting in a high bound for MHHLP. Therefore, this approach is an attempt to find the best bound for the problem to match or close the optimal solution. To create this improvement process, the proposed method of Neamatian Monemi et al. [5] was followed by the sub gradient optimization method. In this method, a six-step algorithm was developed in the form of *Fig. 2*, in which the signs and indexes were used, as follows:

LB: lower bound.

UB: upper bound.

iter: iteration index.

$\tilde{\psi}$: a random response resulting from solving the problem relaxed from hard constraint clause.

LR^{iter} : the output of lagrangian relaxation for the objective function in iter repeat.

π_{iter} : sub gradients of *Constraint (13)* in the iterth iteration.

θ_{iter} : sub gradients of *Constraint (15)* in the iterth iteration.

s_{iter} : the movement step in the iterth iteration.

ρ_{iter} : the multiplicative which is used as a decreasing factor in each iteration.

iter $=0,\ \lambda_{ij-iter}^{kn}=0,\ \mu_{ij-iter}^{kn}=0,\ \rho_{iter}=2,$ *Max.iter*$=100.$

While $\{ s_{iter} \le \varepsilon$ *or* $|UB - LB| \le \varepsilon$ *or* *iter* $\le$ *Max.iter*

Solve RMHHLP (MHHLP without constraints (13) and (15)) and let in $\widetilde{\psi}$;

$LR^{iter} = \widetilde{\psi};$

if $\{ LR^{iter} \le UB$

$UB = LR^{iter};$

else

$\rho_{iter} = 0.9\rho_{iter};$

$\}$

$$\pi_{iter}^{jknj} = x_{ikl}\sum_{\alpha\in I} f_{ia} - w_{ij}^{kn}$$

$$\theta_{iter}^{jknj} = (1-x_{ikl})\sum_{\alpha\in I} f_{ia} - w_{ij}^{kn} - y_{ij}^{in}$$

$$s_{iter} = \frac{\rho_{iter}\left(UB - lr_{iter}\right)}{\sum_{i\in I}\sum_{k\in H}\sum_{l\in H}\sum_{m\in I}\left(\left(\pi_{iter}^{ikmj}\right)^2 + \left(\theta_{iter}^{ikmj}\right)^2\right)};$$

$$\lambda_{ij-iter}^{kn} = max\ \{0,\ \lambda_{ij-iter}^{km} + s_{iter}\pi_{iter}^{ikmj}\};$$

$$\mu_{ij-iter}^{kn} = max\ \{0,\ \mu_{ij-iter}^{km} + s_{iter}\theta_{iter}^{ikmj}\};$$

iter $=$ *iter*$+1$

$\}$

Fig. 2. Optimization subgradients procedure for MHHLP.

In the next section, it is attempted to examine the inequity and proposed method performance, individually and in combination of all available modes with the help of the standard data in the research literature, so that the best combination can be achieved in order to reach the best possible response in the shortest possible time.

4 | ANN Model of the Proposed MHHLP

An information processing system is used in order to predict and estimate the route reliability, or the same value of the MHHLP objective function, which is based on a large number of super-integrated processing elements called neurons that work together to solve a problem and transmit information by synopses (electromagnetic communications); this system is called the ANN in literature and neural biology, which main idea is inspired by the structure of human brain activity [50]. In the last decade, ANN has been used as an effective tool to estimate problems, and given that ANN can be defined as a mathematical system and the neuron is interpreted as a processing unit, network architecture is created helping organizing neurons, many of which are designed in the literature; however, the most popular of them is the Multi-Layer Perceptron (MLP) networks, which are among the Feed Forward Neural Networks type [51].

These networks have input, hidden, and output layers in their topology [28], [51].

The neurons are placed on the layers with an activation function and each neuron is connected to the neurons in the next layer with the weighted connections.

The ANN weights are trained using a form of error feedback, which can be viewed as a generalization of the Learning Management System (LMS) [28].

An error BPA is used to train the network to correct these weights in the various layers of the MLP.

The complexity of the connection network is directly related to the number of layers and neurons of each layer, whose accurate selection has a significant impact on achieving the best possible responses at the best possible time. Therefore, the neural network sensitivity was analyzed based on different numbers of hidden layers, the number of neurons, activation functions, etc. in order to achieve the best topology for MHHLP design, The obtained result is the proposed MLP model structure with four inputs, a hidden layer and an output that is mapped to the CAB dataset in *Fig. 3* and is exactly identical to the IAD dataset, however, 3 neurons are defined instead of the 4 neurons in the hidden layer.

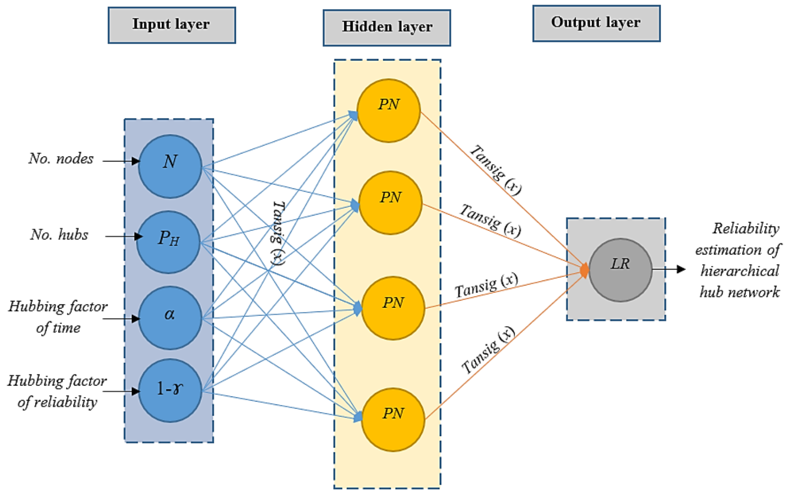

Fig. 3. The proposed MLP model architecture for MHHLP with CAB dataset.

In the context of a feed-forward network, a hidden layer neuron is a Pre-synaptic Neuron (PN) because it is connected to other neurons in the network which are post-synaptic in relation to its output. In feed-forward networks, neurons form layers, or slabs, which are connected to and from post- and pre- synaptic neurons.

Such groupings of neurons that are themselves connected to other neurons are sometimes (traditionally) called hidden layers or hidden layer neurons[1].

Input data is composed of problem parameters (i.e. the number of nodes, the number of hubs, hubbing factor of time and hubbing factor of reliability) and the results of the Lagrangian relaxtion method choosed as output data for training for the ANN model. The Levenberg–Marquardt (LM) algorithm used for the training rule of network. These data were divided into two sets: training set (eighty percent of data) and test set (twenty percent of data). The MATLAB R2013a 8.1.0.604 software used for the training of the ANN model. The implementing phases of the ANN model with BPA presents in the *Fig. 4*. The planned ANN model specifications have been presented in *Table 2* for each data sets of IAD and CAB.

Table 2. The characteristics of planned ANN model.

Neural Network	MLP IAD	CAB
Number of neurons in the input layer	4	4
Number of neurons in the hidden layer	3	4
Number of neurons in the output layer	1	1
Number of epochs	1000	1000
Activation function	Tansig	Tansig

We use tangent sigmoid transfer function tansig function as activation function in MLP models. This function is wellknown in literature [28]. The formulation of Tansig defines in *Eq. (23)* as follow:

$$\operatorname{Tan sig}(x) = \frac{2}{1+\exp-2(x)} - 1. \tag{23}$$

[1] http://standoutpublishing.com/g/hidden-layer.html

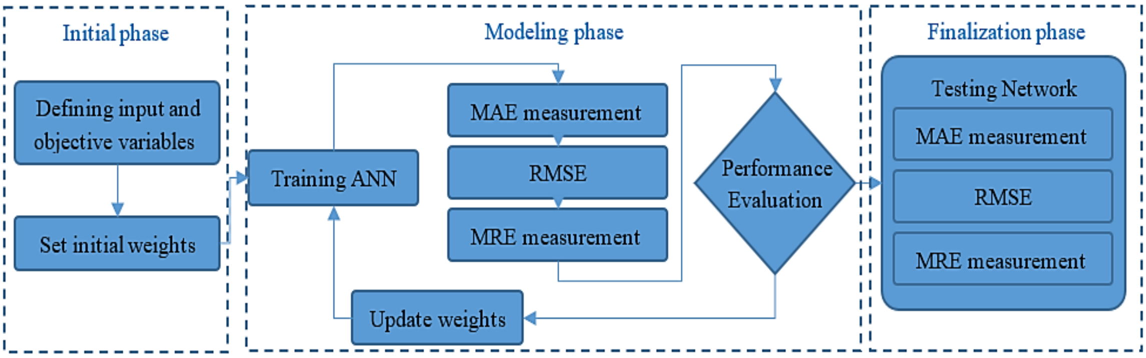

Fig. 4. Flowchart of the ANN model phases (adapted from [51]).

5 | The Computational Results

The present paper uses two well-known dataset in the HLPs literature namely the Civil Aeronautics Board (CAB) and the Iranian Aviation Dataset (IAD). O'kelly [52] introduced the CAB data on the basis of the transport network of the 25 states of the United States.

Karimi and Bashiri [53] studied transportation network in 37 cities of Iran and provided the collected data in the form of IAD. These two data sets do not provide the reliability rate of the routes. Therefore, the reliability of data was adopted from Kim and O'kelly [17] and An et al. [4]. Also, the reciprocating success chance of each return route was assumed equal and, by were placed at a distance of (0,1) by normalizing the reliability data results. The reliability and travel time in the ground mode are reduced by 50% compared to air mode through calculations, considering the capability and ability of air mode to ground mode transportation.

Tehran (the capital city of Iran) was selected as the central hub in the IAD dataset. Placing the only international airport in this city and possessing the largest number of population were the reasons for selecting this city (as the research Alumur et al. [10]). We selected the node 17 with the largest volume of communications (1447732) as the central hub for CAB data in a heuristic attempt regarding the dataset.

The β value is obtained from the average of the problem feasible modes for its various values in the rigorous mode, which is similar to the decision-making process used by Yaman [18], Alumur et al. [14] and Korani Sahraeian [13] to determine β. Therefore, this amount was obtained 2640 and 2880, for the MHHLP structure for CAB and IAD data, respectively.

Three Objective Factor (ObFu), Response Improvement Rate (ReIm) and hub facilities (Hub) were considered to evaluate the performance of the Lagrangian approach. ReIm is obtained from the difference between the pure relaxed response and the lower bound of Lagrangian relaxation on the pure relaxation response.

The numerical initial value ρ_{iter} is considered constant considering the dimensions of the problem. For the subsets 5, 10, 15 and 20, this value was 9, and for the subsets of 25, 30, and 37 nodes, it was considered 90. The results of the Lagrangian relaxation method for IAD and CAB data are presented in Table 3 and *Table 4*, respectively.

Table 3. IAD data with β = 2880.

N	P_H	α	1-ɣ	ObFu	ReIm	Time	Hub
10	3	0.2	0.2	16.254	28.00	76.593	1,9,31
			0.8	13.966	29.00	80.325	3,5,31
		0.8	0.2	16.103	28.00	82.612	2,5,31
			0.8	13.849	29.30	80.150	2,5,31
	6	0.2	0.2	16.966	26.40	76.765	2,4,5,6,7,31
			0.8	14.409	25.80	75.922	2,4,5,6,7,31
		0.8	0.2	16.830	22.30	77.856	1,3,5,7,9,31
			0.8	14.328	26.40	47.638	2,4,6,7,9,31
20	5	0.2	0.2	113.771	22.80	992.932	4,7,9,10,31
			0.8	90.471	15.50	878.752	3,7,13,15,31
		0.8	0.2	113.283	19.10	924.357	1,7,14,18,31
			0.8	90.723	15.90	905.642	4,7,9,10,31
	10	0.2	0.2	108.482	18.80	894.079	4,5,6,9,11,14,15,17,18,31
			0.8	86.561	19.00	877.761	1,3,5,6,9,13,14,17,18,31
		0.8	0.2	107.739	20.90	934.164	1,3,4,6,7,11,13,14,15,31
			0.8	86.498	19.60	915.603	3,5,6,7,9,13,14,15,19,31
30	7	0.2	0.2	308.957	15.30	5369.218	9,23,24,25,27,29,31
			0.8	251.803	18.80	4554.381	7,9,11,14,21,24,31
		0.8	0.2	306.568	15.90	4031.185	5,6,9,12,14,27,31
			0.8	249.149	19.70	3699.427	9,14,16,19,20,28,31
	14	0.2	0.2	295.254	18.40	5355.854	3,6,8,9,12,14,15,17,18,21,24,28,29,31
			0.8	237.440	21.80	5845.368	4,6,8,9,11,13,14,17,18,20,21,24,26,31
		0.8	0.2	294.495	18.60	5425.368	1,4,5,6,8,9,14,15,16,17,19,21,27,31
			0.8	238.374	21.50	5326.301	5,6,8,9,14,16,17,18,21,23,26,28,29,31
37	9	0.2	0.2	518.064	12.01	19527.866	2,3,9,24,27,31,33,34,37
			0.8	415.573	16.00	17651.638	1,9,13,17,22,26,31,33,34
		0.8	0.2	205.762	11.84	17561.843	8,9,14,17,18,24,31,35,37
			0.8	413.988	16.30	13816.276	3,9,11,24,26,29,31,33,37
	18	0.2	0.2	498.805	20.48	21220.677	2,5,6,7,8,9,13,14,20,21,25,26,31,33,34,35,36,37
			0.8	383.840	20.48	23277.403	2,5,6,7,8,9,13,14,20,21,25,26,31,33,34,35,36,37
		0.8	0.2	484.755	20.48	21729.580	2,5,6,7,8,9,13,14,20,21,25,26,31,33,34,35,36,37
			0.8	383.980	20.48	20924.306	2,5,6,7,8,9,13,14,20,21,25,26,31,33,34,35,36,37

Table 4. CAB data with β = 2640.

N	P_H	α	1-ɤ	ObFu	ReIm	Time	Hub
5	1	0.2	0.2	1234845.515988	36.40	26.735	17
			0.8	1170003.494381	35.30	27.629	17
		0.8	0.2	1234845.515988	36.40	25.775	17
			0.8	1170003.494381	35.30	28.521	17
	3	0.2	0.2	1470844.172062	23.60	29.993	3,4,17
			0.8	1375857.385783	22.90	31.513	1,3,17
		0.8	0.2	1470844.172062	23.60	30.972	3,4,17
			0.8	1375857.385783	22.90	29.933	1,3,17
15	4	0.2	0.2	8581277.210319	19.40	303.486	3,9,12,17
			0.8	6927494.390239	21.80	298.223	9,12,14,17
		0.8	0.2	8344651.530996	21.60	293.957	6,8,12,17
			0.8	6944090.143229	20.90	290.832	2,8,12,17
	8	0.2	0.2	8302771.440473	21.70	316.900	6,7,8,10,11,12,13,17
			0.8	6683215.422164	23.20	296.309	2,3,5,6,8,13,14,17
		0.8	0.2	8184242.793126	22.80	305.893	1,3,4,8,12,13,14,17
			0.8	6649183.937808	23.10	283.404	1,2,4,11,12,13,14,17
25	6	0.2	0.2	25413461.934842	11.90	3835.420	13,16,17,19,20,23
			0.8	20202865.443763	14.30	2876.640	2,3,8,17,19,24
		0.8	0.2	25109500.301100	12.80	2020.928	5,12,17,19,22,23
			0.8	20236900.452763	13.60	3476.640	9,11,17,19,22,23,
	12	0.2	0.2	24983278.442424	12.90	3132.293	7,8,10,11,13,15,16,17,18,19,21,23
			0.8	19702691.089243	14.70	2601.043	1,2,3,5,9,10,13,14,17,19,22,23
		0.8	0.2	24774015.368644	13.50	1940.601	7,8,10,11,13,15,17,18,19,21,22,23
			0.8	19478500.521147	15.20	2104.402	2,6,8,11,12,13,16,17,19,22,23,24

To demonstrate the impressionability of the ObFu and step size changes process from ρ_{iter} , *Fig. 5* is plotted for the 30-node set of IAD data, so that PH = 7, = 0.8 and = 0.8 α, by GAMS software outputs. *Fig. 5* shows that the accuracy of the calculation is greater by increasing the discount factor in large data and the changes curve is more concave, and vice versa, the change slope of step size changes shifted from line shape to stairs, which guarantees achieving the better response.

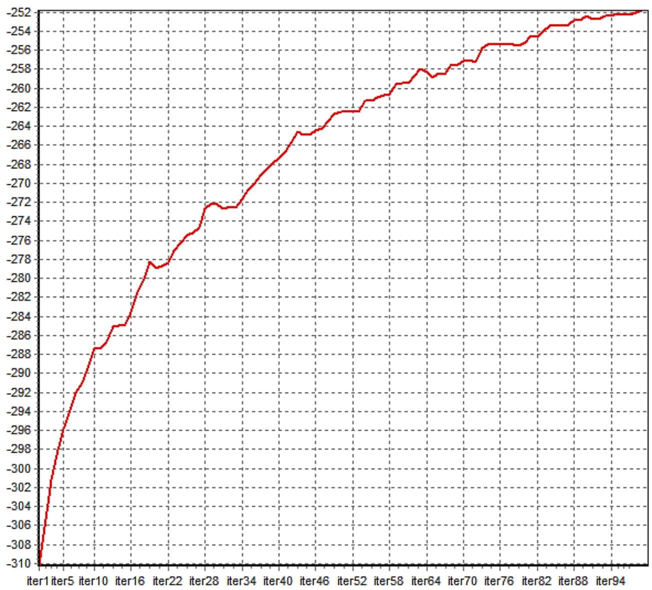

a.

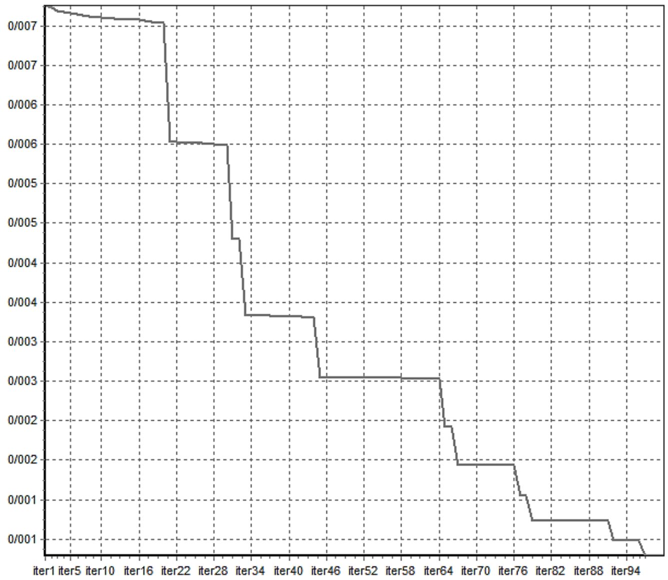

b.

Fig. 5. Trends of ObFu; a) and step size, b) for IAD dataset with PH=7, $\rho_{iter} = 90$, α=0.8 and ϒ =0.8.

Table 5 and *Table 6* show the obtained results for the proposed ANN model for IAD and CAB datasets, respectively. So that, the *Eqs. (24)-(26)* are used to calculating the mean relative error percentage (MRE %), the Root Means Square Error (RMSE) and the mean absolute error percentage (MAE %) of the network, respectively.

$$MRE\% = 100 \times \frac{1}{N} \sum_{i=1}^{N} \left| \frac{x_i(\exp) - x_i(\text{pred})}{x_i(\exp)} \right|. \quad (24)$$

$$RMSE = \sqrt{\frac{\sum_{i=1}^{N} (x_i(\exp) - x_i(\text{pred}))^2}{N}}. \quad (25)$$

$$MAE\% = 100 \times \frac{1}{N} \sum_{i=1}^{N} \left| x_i(\exp) - x_i(\text{pred}) \right|. \quad (26)$$

Table 5. The training and testing errors results of the proposed ANN model for IAD data.

Error	Train	Test
MRE%	1.4122	2.6311
RMSE	0.0033	0.0045
MAE%	0.2089	0.2722

Table 6. The training and testing errors results of the proposed ANN model for CAB data.

Error	Train	Test
MRE%	0.0016	0.1391
RMSE	1.39×10^{-5}	4.41×10^{-4}
MAE%	4.1×10^{-4}	0.0238

All of the symbols and indexes are used in the *Eqs. (24)-(26)*, define in *Table 7*.

Table 7. The symbols in the Eqs. (24)-(26).

Symbol	Definition
N	The number of data
x(exp)	Stand for real ANN values
x(pred)	Stand for predicted ANN values

Several numbers of neurons have been applied for the proposed ANN architectures, which best structure is selected. The results of the applied networks with different number of neurons in the hidden layer are illustrated in *Fig. 6*. This figure shows the MAE errors of the networks versus different number of neurons in the hidden layer. Each point in these figure represent the network with best MAE results during 200 times. These MAE errors are reported according to the normalized data.

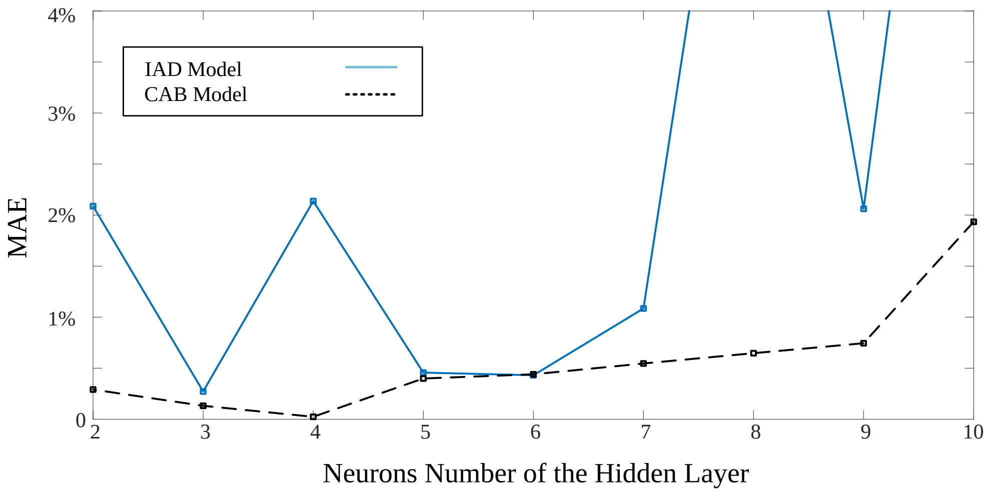

Fig. 6. MAE errors of the networks versus different number of neurons in the hidden layer.

According to *Fig. 6*, the numbers of 3 and 4 neurons, which have the best MAE error values, are considered for the hidden layers of IAD and CAB models, respectively. In the proposed networks, 80 percent of data set is used for training, while 20 percent of the data set is used for testing process of the presented model. So, we suggested ANN model for both datasets then train and test for everyone. Objective function actual and predicted values comparison for the IAD data, using the proposed MLP model for IAD is illustrated in *Fig. 7* and *Fig. 8*. The objective function actual and predicted data for training and testing process for IAD data are listed in *Table 8* and *Table 9*, respectively. Also, the conformity actual and predicted values for the IAD data using the proposed MLP model for IAD are illustrated in *Fig. 8*.

As can be seen from *Fig. 7* and *Fig. 8* and *Table 8* and *Table 9*, the test and train data are predicted precisely and the predicted values of output MHHLP reliability by ANN model is the instances of near to the Objective function actual results, undoubtedly.

The outcomes endorse the accuracy and applicability of estimation of ANN as a reliable model to predict the proposed MLPs output MHHLP reliability from the number of nodes, the number of hubs, hubbing factor of time and hubbing factor of reliability validate by results.

Table 8. Model results for IAD train data with β = 2880.

Input				Output	
N	PH	α	1-ɤ	Actual	Predicted
30	14	0.2	0.8	237.44	239.62
20	10	0.8	0.8	86.50	85.63
10	6	0.2	0.8	14.41	13.48
37	9	0.8	0.8	413.99	413.99
20	5	0.8	0.2	113.28	113.21
37	9	0.2	0.2	518.06	513.10
30	7	0.8	0.8	249.15	249.26
30	7	0.2	0.2	308.96	311.85
37	9	0.8	0.2	205.76	205.76
37	18	0.8	0.2	484.75	484.76
10	6	0.2	0.2	16.97	17.41
20	10	0.8	0.2	107.74	107.67
30	14	0.8	0.8	238.37	239.96
30	14	0.8	0.2	294.5	293.92
37	18	0.2	0.2	498.8	500.78
20	5	0.2	0.8	90.47	91.13
37	18	0.2	0.8	383.84	383.85
10	3	0.2	0.8	13.97	13.96
30	14	0.2	0.2	295.25	292.29
10	3	0.8	0.2	16.10	17.85
20	10	0.2	0.2	108.48	108.51
10	6	0.8	0.8	14.33	13.33
20	10	0.2	0.8	86.56	86.48
30	7	0.2	0.8	251.80	248.67
30	7	0.8	0.2	306.57	306.59

Table 9. Model results for IAD test data with β = 2880.

Input				Output	
N	P_H	α	1-ɤ	Actual	Predicted
37	9	0.2	0.8	415.57	420.84
10	3	0.2	0.2	16.25	18.06
10	3	0.8	0.8	13.85	13.80
20	5	0.2	0.2	113.77	114.03
20	5	0.8	0.8	90.72	90.26
10	6	0.8	0.2	16.83	17.21

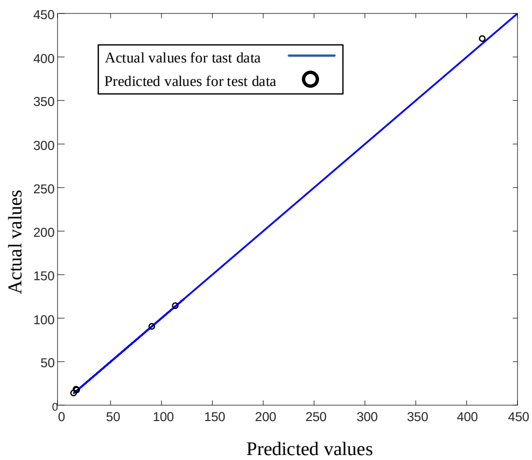

a.

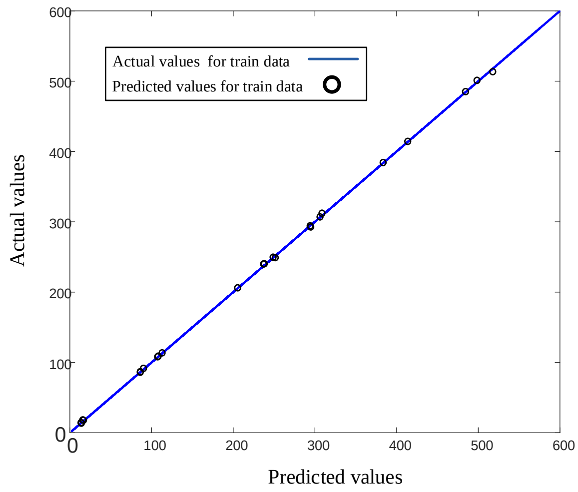

b.

Fig. 7. Actual and predicted values comparison of; a) test and, b) train data, using the proposed MLP model for IAD.

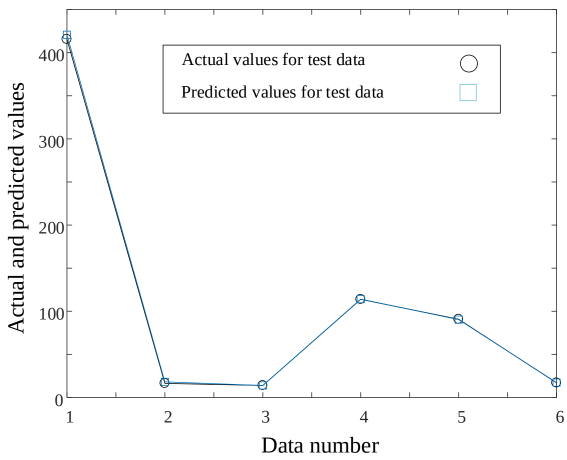

a.

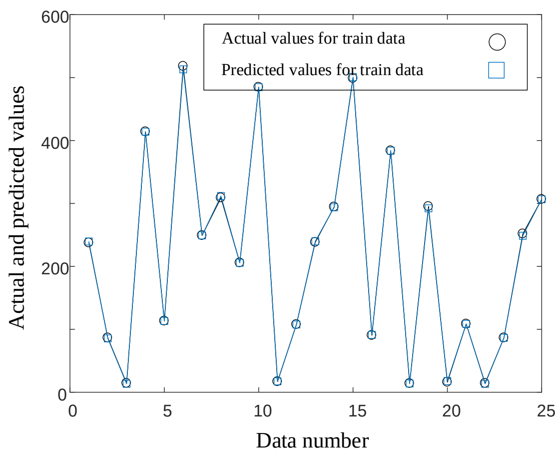

b.

Fig. 8. Conformity actual and predicted values of; a) test and, b) train data, using the proposed MLP model for IAD.

Another model is propped for the CAB data. Actual and predicted values comparison for the CAB data, using the proposed MLP model for CAB is illustrated in *Fig. 9* and *Fig. 10*. The objective function actual and predicted data for training and testing process for CAB data are listed in *Table 10* and *Table 11*, respectively. As can be seen, the test and train data are predicted precisely.

Also, the conformity actual and predicted values for the CAB data using the proposed MLP model for CAB are illustrated in *Fig. 10*.

Table 10. Model results for CAB train data with β = 2640.

Input				Output	
N	P_H	α	1-ɤ	Actual	Predicted
25	6	0.2	0.2	25413461.9	25412043.2
25	12	0.8	0.2	24774015.3	24773994.9
5	1	0.2	0.2	1234845.52	1234990.91
5	1	0.8	0.2	1234845.52	1234701.76
5	3	0.2	0.8	1375857.39	1375855.70
15	4	0.2	0.2	8581277.21	8581269.82
15	8	0.20	0.2	8302771.44	8302775.49
25	12	0.20	0.8	19702691.0	19702692.5
15	8	0.80	0.8	6649183.94	6649185.67
15	4	0.20	0.8	6927494.39	6927494.40
15	8	0.20	0.8	6683215.42	6683216.26
15	8	0.80	0.2	8184242.79	8184243.93
25	6	0.80	0.8	20236900.4	20236900.5
15	4	0.80	0.2	8344651.53	8344658.59
5	1	0.80	0.8	1170003.49	1170003.39
25	6	0.20	0.8	20202865.4	20202865.1
25	12	0.20	0.2	24983278.4	24983308.4
25	6	0.80	0.2	25109500.3	25109509.2

Table 11. Model results for CAB test data with β = 2640.

Input				Output	
N	P_H	α	1-ɤ	Actual	Predicted
15	4	0.80	0.80	6944090.14	6920353.81
5	1	0.20	0.80	1170003.49	1169883.82
5	3	0.80	0.80	1375857.39	1374359.18
5	3	0.20	0.20	1470844.17	1473467.30
5	3	0.80	0.20	1470844.17	1470019.09

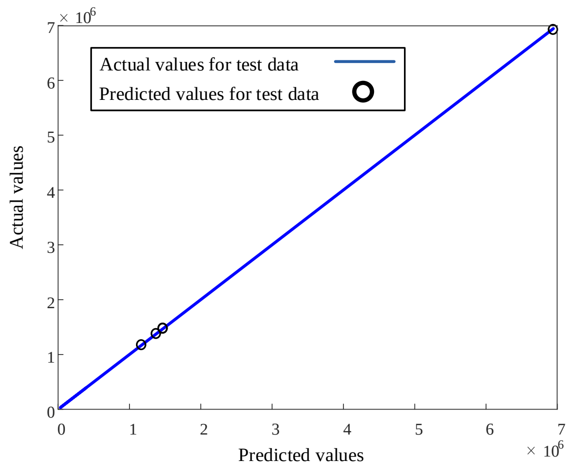

a.

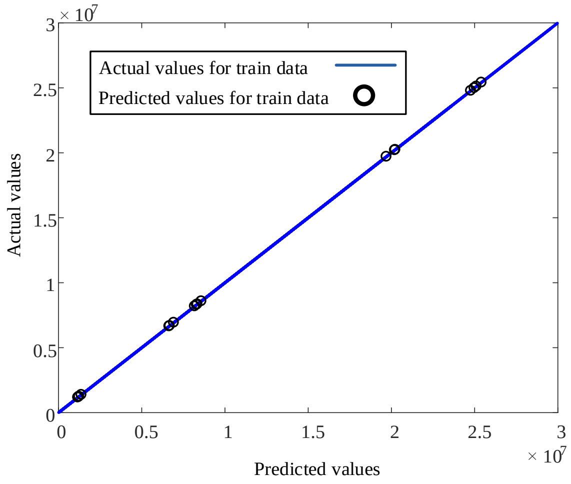

b.

Fig. 9. Actual and predicted values comparison of; a) test and, b) train data, using the proposed CAB-MLP model.

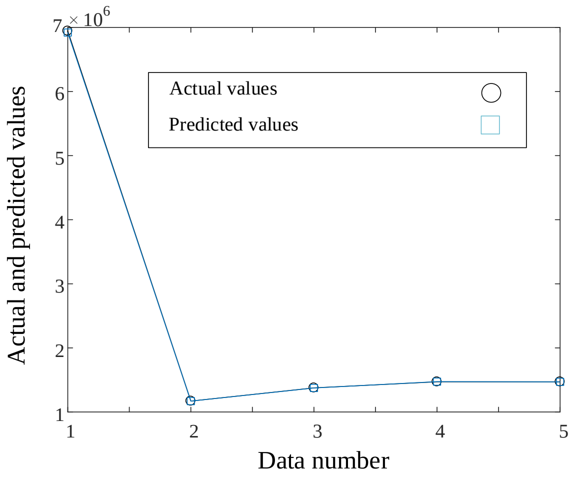

a.

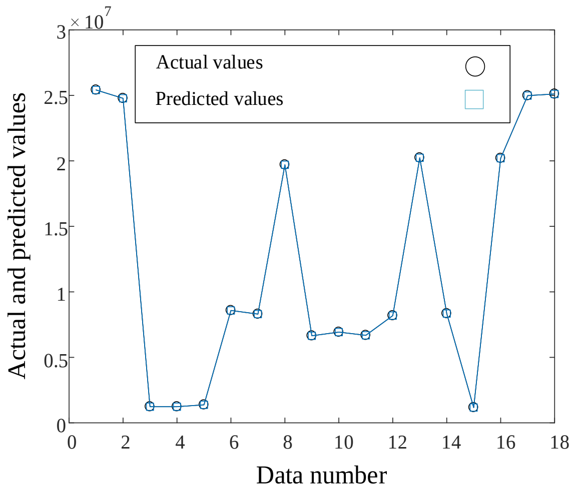

b.

Fig. 10. Conformity actual and predicted values of; a) test and, b) train data, using the proposed MLP model for CAB data.

The most important benefits of the proposed ANN model are the ease of use, present output at the best time and the quality of the solution. Accordingly, the MHHLP reliability for the IAD with N=37 and CAB with N=25 was predicted that the different values of the three inputs PH, 1- ɤ and α. Hence, the following data are predicted by the proposed IAD and CAB MLP models which are listed in *Table 12* and *Table 13*, respectively. These results have been calculated in best time vs solution time other methods.

Table 12. Predicted results of MLP model for IAD data.

	Input			Output	Input			Output
N	P_H	α	1-ɤ	Predicted	P_H	α	1-ɤ	Predicted
37	4	0.20	0.2	516.41	20	0.80	0.2	270.50
	4	0.20	0.8	445.72	20	0.80	0.8	412.28
	4	0.80	0.2	245.55	24	0.20	0.2	509.71
	4	0.80	0.8	355.12	24	0.20	0.8	406.71
	8	0.20	0.2	515.67	24	0.80	0.2	367.01
	8	0.20	0.8	438.06	24	0.80	0.8	407.71
	8	0.80	0.2	193.45	28	0.20	0.2	507.23
	8	0.80	0.8	394.87	28	0.20	0.8	398.95
	12	0.20	0.2	514.68	28	0.80	0.2	436.85
	12	0.20	0.8	430.27	28	0.80	0.8	401.67
	12	0.80	0.2	170.19	32	0.20	0.2	504.26
	12	0.80	0.8	410.13	32	0.20	0.8	391.32
	16	0.20	0.2	513.39	32	0.80	0.2	471.05
	16	0.20	0.8	422.41	32	0.80	0.8	394.91
	16	0.80	0.2	194.30	36	0.20	0.2	500.78
	16	0.80	0.8	414.00	36	0.20	0.8	383.85
	20	0.20	0.2	511.75	36	0.80	0.2	484.76
	20	0.20	0.8	414.54	36	0.80	0.8	387.84

Table 13. Predicted results of MLP model for CAB data.

	Input			Output				Output
N	P_H	α	1-ɤ	Predicted	P_H	α	1-ɤ	Predicted
25	1	0.2	0.2	25050451.39	15	0.2	0.2	25406442.84
	1	0.2	0.8	16026295.13	15	0.2	0.8	15325554.90
	1	0.8	0.2	19377456.30	15	0.8	0.2	25004882.77
	1	0.8	0.8	15962120.70	15	0.8	0.8	13761050.31
	5	0.2	0.2	25398242.67	20	0.2	0.2	25258947.23
	5	0.2	0.8	19560692.82	20	0.2	0.8	5498956.327
	5	0.8	0.2	23516098.44	20	0.8	0.2	24700271.80
	5	0.8	0.8	19437441.01	20	0.8	0.8	17857038.8
	10	0.2	0.2	25412159.53	25	0.2	0.2	24983308.43
	10	0.2	0.8	20975665.79	25	0.2	0.8	19702692.57
	10	0.8	0.2	25045876.39	25	0.8	0.2	24773994.90
	10	0.8	0.8	20904014.18	25	0.8	0.8	21716295.3

6 | Conclusions

The gap is determined in this paper through examining the literature on HLPs and a new model called MHHLP was introduced, which included three multimodal transport, hierarchical structure and reliability characteristics, simultaneously. The contribution of the proposed model is in terms of its constraints and problem variables design and that, the different routes of network are identified and formulated based on the demand flow in the network in defining its equations. Considering the problem placement in the range of NP-Hard problems, the Lagrangian Relaxation Algorithm was developed for it and the results were obtained, accordingly. Finally, the data gathered by the Multilayer Perceptron (MLP) neural network were transformed into a model.

Therefore, this paper has been presented a new feedforward method for estimating the reliability of MHHLP. For validation, the output reliability was predicted using proposed ANN model for the MHHLP. This proposed method is easily estimated the reliability of the MHHLP and has been validated by ANN model. Hence, the presented ANN model can be applied instead of the MHHLP model, for other implementations.

Acknowledgments

The author would like to express sincere gratitude to all those who contributed to this research, including colleagues and mentors for their valuable insights and constructive feedback.

Funding

This research received no specific grant from any funding agency in the public, commercial, or not-for-profit sectors.

Data Availability

The data used in this study, including the CAB and IAD datasets, are publicly available and have been obtained from previously published sources. Any additional data or computational models generated during this research can be made available upon reasonable request to the corresponding author.

References

[1] Farahani, R. Z., Hekmatfar, M., Arabani, A. B., & Nikbakhsh, E. (2013). Hub location problems: A review of models, classification, solution techniques, and applications. *Computers and industrial engineering*, *64*(4), 1096–1109. https://doi.org/10.1016/j.cie.2013.01.012

[2] Teo, C. P., & Shu, J. (2004). Warehouse-retailer network design problem. *Operations research*, *52*(3), 396–408. https://doi.org/10.1287/opre.1030.0096

[3] Jia, H., Ordóñez, F., & Dessouky, M. (2007). A modeling framework for facility location of medical services for large-scale emergencies. *IIE transactions*, *39*(1), 41–55. https://doi.org/10.1080/07408170500539113

[4] An, Y., Zhang, Y., & Zeng, B. (2015). The reliable hub-and-spoke design problem: models and algorithms. *Transportation research part b: methodological*, *77*, 103–122. https://doi.org/10.1016/j.trb.2015.02.006

[5] Neamatian Monemi, R., Gelareh, S., Hanafi, S., & Maculan, N. (2017). A co-opetitive framework for the hub location problems in transportation networks. *Optimization*, *66*(12), 2089–2106. https://doi.org/10.1080/02331934.2017.1295045

[6] Correia, I., Nickel, S., & Saldanha-da-Gama, F. (2018). A stochastic multi-period capacitated multiple allocation hub location problem: formulation and inequalities. *Omega*, *74*, 122–134. https://doi.org/10.1016/j.omega.2017.01.011

[7] Martins de Sá, E., Morabito, R., & de Camargo, R. S. (2018). Benders decomposition applied to a robust multiple allocation incomplete hub location problem. *Computers and operations research*, *89*, 31–50. https://doi.org/10.1016/j.cor.2017.08.001

[8] Revelle, C. S., Eiselt, H. A., & Daskin, M. S. (2008). A bibliography for some fundamental problem categories in discrete location science. *European journal of operational research*, *184*(3), 817–848. https://doi.org/10.1016/j.ejor.2006.12.044

[9] Melo, M. T., Nickel, S., & Saldanha-Da-Gama, F. (2009). Facility location and supply chain management--A review. *European journal of operational research*, *196*(2), 401–412. https://doi.org/10.1016/j.ejor.2008.05.007

[10] Gelareh, S., Nickel, S., & Pisinger, D. (2010). Liner shipping hub network design in a competitive environment. *Transportation research part e: logistics and transportation review*, *46*(6), 991–1004. https://doi.org/10.1016/j.tre.2010.05.005

[11] Gelareh, S., & Nickel, S. (2011). Hub location problems in transportation networks. *Transportation research part e: logistics and transportation review*, *47*(6), 1092–1111. https://doi.org/10.1016/j.tre.2011.04.009

[12] Yaman, H., & Elloumi, S. (2012). Star p-hub center problem and star p-hub median problem with bounded path lengths. *Computers and operations research*, *39*(11), 2725–2732. https://doi.org/10.1016/j.cor.2012.02.005

[13] Korani, E., & Sahraeian, R. (2013). The hierarchical hub covering problem with an innovative allocation procedure covering radiuses. *Scientia Iranica*, *20*(6), 2138–2160. https://scientiairanica.sharif.edu/article_3452.html

[14] Alumur, S. A., Yaman, H., & Kara, B. Y. (2012). Hierarchical multimodal hub location problem with time-definite deliveries. *Transportation research part e: logistics and transportation review*, *48*(6), 1107–1120. https://doi.org/10.1016/j.tre.2012.04.001

[15] Karimi, H., & Setak, M. (2014). Proprietor and customer costs in the incomplete hub location-routing network topology. *Applied mathematical modelling*, *38*(3), 1011–1023. https://doi.org/10.1016/j.apm.2013.07.033

[16] Snyder, L. V., Atan, Z., Peng, P., Rong, Y., Schmitt, A. J., & Sinsoysal, B. (2016). OR/MS models for supply chain disruptions: A review. *IIE transactions (institute of industrial engineers)*, *48*(2), 89–109. https://doi.org/10.1080/0740817X.2015.1067735

[17] Kim, H., & O'Kelly, M. E. (2009). Reliable p-hub location problems in telecommunication networks. *Geographical analysis*, *41*(3), 283–306. https://doi.org/10.1111/j.1538-4632.2009.00755.x

[18] Yaman, H. (2009). The hierarchical hub median problem with single assignment. *Transportation research part b: methodological*, *43*(6), 643–658. https://doi.org/10.1016/j.trb.2009.01.005

[19] Chopra, S., & Meindl, P. (2007). Supply chain management. Strategy, planning & operation. In *Das summa summarum des management*. Gabler. https://doi.org/10.1007/978-3-8349-9320-5_22

[20] Chen, S., Yan, Y., & Song, H. (2010). Optimal logistics hubs locations on the multimodal transportation network. In *ICLEM 2010: logistics for sustained economic development: infrastructure, information, integratio* (Vol. 387, pp. 2853–2858). https://doi.org/10.1061/41139(387)399

[21] Onyemechi, C. (2010). Regional hubs and multimodal logistics efficiency in the 21st century. *Journal of maritime research*, *7*(2), 63–72.

[22] SteadieSeifi, M., Dellaert, N., & Woensel, T. Van. (2014). A multimodal network flow problem with product quality preservation, transshipment, and asset management. *Industrial engineering and innovation sciences*, *442*(January). http://cms.ieis.tue.nl/Beta/Files/WorkingPapers/wp_442.pdf

[23] Hanasusanto, G. A., Kuhn, D., Wallace, S. W., & Zymler, S. (2015). Distributionally robust multi-item newsvendor problems with multimodal demand distributions. *Mathematical programming*, *152*(1–2), 1–32. https://doi.org/10.1007/s10107-014-0776-y

[24] Ambrosino, D., & Sciomachen, A. (2016). A capacitated hub location problem in freight logistics multimodal networks. *Optimization letters*, *10*(5), 875–901. https://doi.org/10.1007/s11590-016-1022-8

[25] Fazayeli, S., Eydi, A., & Kamalabadi, I. N. (2018). A model for distribution centers location-routing problem on a multimodal transportation network with a meta-heuristic solving approach. *Journal of industrial engineering international*, *14*(2), 327–342. https://doi.org/10.1007/s40092-017-0218-6

[26] Huang, D., Liu, Z., Fu, X., & Blythe, P. T. (2018). Multimodal transit network design in a hub-and-spoke network framework. *Transportmetrica a: transport science*, *14*(8), 706–735. https://doi.org/10.1080/23249935.2018.1428234

[27] Yuan, X. H., & Feng, Q. Y. (2012). Behavioral modeling of RF power amplifiers with memory effects using orthonormal hermite polynomial basis neural network. *Progress in electromagnetics research c*, *34*, 239–251. https://doi.org/10.2528/pierc12091903

[28] Hayati, M., Shama, F., Roshani, S., & Abdipour, A. (2014). Linearization design method in class-F power amplifier using artificial neural network. *Journal of computational electronics*, *13*(4), 943–949. https://doi.org/10.1007/s10825-014-0612-x

[29] Leśniak, A., & Juszczyk, M. (2018). Prediction of site overhead costs with the use of artificial neural network based model. *Archives of civil and mechanical engineering*, *18*(3), 973–982. https://doi.org/10.1016/j.acme.2018.01.014

[30] Strąkowski, R., Pacholski, K., Więcek, B., Olbrycht, R., Wittchen, W., & Borecki, M. (2018). Estimation of FeO content in the steel slag using infrared imaging and artificial neural network. *Measurement*, *117*, 380–389. https://doi.org/10.1016/j.measurement.2017.12.031

[31] Cooper, S. B., & DiMaio, D. (2018). Static load estimation using artificial neural network: application on a wing rib. *Advances in engineering software*, *125*, 113–125. https://doi.org/10.1016/j.advengsoft.2018.01.007

[32] Park, S., Kim, M., Kim, M., Namgung, H. G., Kim, K. T., Cho, K. H., & Kwon, S. B. (2018). Predicting PM10 concentration in Seoul metropolitan subway stations using artificial neural network (ANN). *Journal of hazardous materials*, *341*, 75–82. https://doi.org/10.1016/j.jhazmat.2017.07.050

[33] Sebaaly, H., Varma, S., & Maina, J. W. (2018). Optimizing asphalt mix design process using artificial neural network and genetic algorithm. *Construction and building materials*, *168*, 660–670. https://doi.org/10.1016/j.conbuildmat.2018.02.118

[34] Romański, L., Bieniek, J., Komarnicki, P., Dębowski, M., & Detyna, J. (2017). Estimation of operational parameters of the counter-rotating wind turbine with artificial neural networks. *Archives of civil and mechanical engineering*, *17*(4), 1019–1028. https://doi.org/10.1016/j.acme.2017.04.010

[35] Zavrtanik, N., Prosen, J., Tušar, M., & Turk, G. (2016). The use of artificial neural networks for modeling air void content in aggregate mixture. *Automation in construction*, *63*, 155–161. https://doi.org/10.1016/j.autcon.2015.12.009

[36] Kristjanpoller, W., & Minutolo, M. C. (2015). Gold price volatility: A forecasting approach using the Artificial Neural Network--GARCH model. *Expert systems with applications*, *42*(20), 7245–7251. https://doi.org/10.1016/j.eswa.2015.04.058

[37] Emamgholizadeh, S., Parsaeian, M., & Baradaran, M. (2015). Seed yield prediction of sesame using artificial neural network. *European journal of agronomy*, *68*, 89–96. https://doi.org/10.1016/j.eja.2015.04.010

[38] Skorin-Kapov, D., Skorin-Kapov, J., & O'Kelly, M. (1996). Tight linear programming relaxations of uncapacitated p-hub median problems. *European journal of operational research*, *94*(3), 582–593. https://doi.org/10.1016/0377-2217(95)00100-X

[39] Correia, I., Nickel, S., & Saldanha-da-Gama, F. (2010). The capacitated single-allocation hub location problem revisited: A note on a classical formulation. *European journal of operational research*, *207*(1), 92–96. https://doi.org/10.1016/j.ejor.2010.04.015

[40] Ernst, A. T., & Krishnamoorthy, M. (1999). Solution algorithms for the capacitated single allocation hub location problem. *Annals of operations research*, *86*(0), 141–159. https://doi.org/10.1023/a:1018994432663

[41] Ebery, J. (2001). Solving large single allocation p-hub problems with two or three hubs. *European journal of operational research*, *128*(2), 447–458. https://doi.org/10.1016/S0377-2217(99)00370-7

[42] Ernst, A. T., Jiang, H., Krishnamoorthy, M., Baatar, D., Judge, C., & others. (2005). Reformulations and computational results for uncapacitated single and multiple allocation hub covering problems. *Unpublished report, csiro mathematical and information sciences, australia*. B2n.ir/n97617

[43] Aykin, T. (1994). Lagrangian relaxation based approaches to capacitated hub-and-spoke network design problem. *European journal of operational research*, *79*(3), 501–523. https://doi.org/10.1016/0377-2217(94)90062-0

[44] Lee, Y., Lim, B. H., & Park, J. S. (1996). A hub location problem in designing digital data service networks: lagrangian relaxation approach. *Location science*, *4*(3), 185–194. https://doi.org/10.1016/S0966-8349(96)00009-5

[45] Marín, A. (2005). Uncapacitated euclidean hub location: Strengthened formulation, new facets and a relax-and-cut algorithm. *Journal of global optimization*, *33*(3), 393–422. https://doi.org/10.1007/s10898-004-6099-4

[46] Contreras, I., Díaz, J. A., & Fernández, E. (2009). Lagrangean relaxation for the capacitated hub location problem with single assignment. *OR spectrum*, *31*(3), 483–505. https://doi.org/10.1007/s00291-008-0159-y

[47] Ishfaq, R., & Sox, C. R. (2011). Hub location-allocation in intermodal logistic networks. *European journal of operational research*, *210*(2), 213–230. https://doi.org/10.1016/j.ejor.2010.09.017

[48] Mohammadi, M., Torabi, S. A., & Tavakkoli-Moghaddam, R. (2014). Sustainable hub location under mixed uncertainty. *Transportation research part e: logistics and transportation review*, *62*, 89–115. https://doi.org/10.1016/j.tre.2013.12.005

[49] He, Y., Wu, T., Zhang, C., & Liang, Z. (2015). An improved MIP heuristic for the intermodal hub location problem. *Omega (united kingdom)*, *57*, 203–211. https://doi.org/10.1016/j.omega.2015.04.016

[50] Haykin, S. (1994). *Neural Networks: A Comprehensive Foundation*. Prentice Hall PTR. https://dl.acm.org/doi/abs/10.5555/541500

[51] Khoshroo, A., Emrouznejad, A., Ghaffarizadeh, A., Kasraei, M., & Omid, M. (2018). Sensitivity analysis of energy inputs in crop production using artificial neural networks. *Journal of cleaner production*, *197*, 992–998. https://doi.org/10.1016/j.jclepro.2018.05.249

[52] O'kelly, M. E. (1987). A quadratic integer program for the location of interacting hub facilities. *European journal of operational research*, *32*(3), 393–404. https://doi.org/10.1016/S0377-2217(87)80007-3

[53] Karimi, H., & Bashiri, M. (2011). Hub covering location problems with different coverage types. *Scientia iranica*, *18*(6), 1571–1578. https://doi.org/10.1016/j.scient.2011.09.018